FACTA UNIVERSITATIS
Series: **Mechanical Engineering**
https://doi.org/10.22190/FUME210106020K

Original scientific paper

ON THE INFLUENCE OF MULTIPLE EQUILIBRIUM POSITIONS ON BRAKE NOISE

Sebastian Koch, Emil Köppen, Nils Gräbner, Utz von Wagner

Chair of Mechatronics and Machine Dynamics, Technische Universität Berlin, Germany

Abstract. *Brake noise, especially brake squeal, has been a subject of intensive research both in industry and academia for several decades. Nevertheless, the state of the art simulations does not provide a predictive tool, and extensive experimental investigations are still necessary to find an appropriate design. Actual investigations focus on the consideration of nonlinearities which are in fact essential for this phenomenon. Unfortunately, by far not all relevant effects caused by nonlinearities are known. One of these nonlinear effects that the actual research focuses on is the limit cycle behavior representing squeal. In contrast to this, the actual paper considers the influence of the equilibrium position established while applying the brake pressure. The elements of the brake, namely, the carrier, caliper and pad, are highly nonlinear and elastically coupled and allow for multiple equilibrium positions depending e.g. on the initial conditions and transient application of the brake pressure while the frictional contact between the pads and the disk may excite small amplitude self-excited vibrations around this equilibrium, i.e. squeal. The current paper establishes a method and corresponding setup, to measure the position engaged by the brake components using an optical 3D-measuring system. Subsequently, it is demonstrated that in fact different equilibrium positions can be engaged for the same operation parameters and that the engaged position can be decisive for the occurrence of squeal. In fact, certain positions result in squeal while others do not for the same operation parameters. Taking this effect into consideration may have significant consequences for the design of brakes as well as simulation and experimental investigation of brake squeal.*

Key Words: *Brake Noise, Nonlinearities, Equilibrium Positions, Digital Image Correlation*

1. INTRODUCTION

Brake squeal and other brake noises are typical examples for NVH (Noise, Vibration, Harshness) problems in the automotive industry. These phenomena in general do not

Received January 06, 2021 / Accepted February 15, 2021
Corresponding author: Sebastian Koch
Chair of Mechatronics and Machine Dynamics, Technische Universität Berlin, Einsteinufer 5, 10587 Berlin
E-mail: koch@tu-berlin.de

represent safety risks but are merely comfort issues. Their avoidance nevertheless requires a considerable amount of development and testing, making brake noise a topic of numerous scientific and technical publications. Several review papers, e.g. [1] and [2], provide overviews on the topic.

The brake squeal simulation is still a tool with only a limited predictive character which almost always requires, in addition, experimental investigations. It is well known that the alteration of operating parameters such as brake pressure, brake torque, speed or brake disk temperature during such experiments has a strong influence on the squealing behavior, see e.g. [3]. Therefore, the necessary number of tests to classify the brake in such manner is extensive, e.g. [4]. The situation becomes more complicated by the fact that there is a possibility for squealing to sometimes occur and sometimes not even during the tests with the identical operation parameters [5-7]. Ref. [6] mainly considers thereby changes in the direction in which the brake components obviously capture significantly different positions as well as the corresponding influence on the squealing behavior.

The state of the art procedure to experimentally classify the squealing behavior of the passenger car brakes is SAE J2521. During this test, the entire brake and the wheel suspension are mounted on a dynamo test bench. A huge amount of braking operations is performed on different parameters, while the noise level is recorded to categorize whether the brake is squealing or not.

On the other hand, the industrial state of the art for the brake squeal simulation is based on the consideration of simulation data gathered from Finite Element (FE) models. The analysis is divided into multiple steps [8]. In the first step, the brake pressure is applied quasi statically to determine the equilibrium position and the contact forces. Therefore, a nonlinear contact analysis is used. Then the model is linearized with respect to the found equilibrium position. Obviously, the equations of motion of this linearized model depend on this equilibrium position. The linear model is finally used for a complex eigenvalue analysis (CEA). Since these models contain, if correctly set up, the mechanism of self-excitation due to the friction forces between the disk and the pad, there is a possibility of instability of the equilibrium position and the mode shapes with eigenvalues with a positive real part are considered as modes potentially associated with squealing [9]. However, linear instability does not represent the observed behavior of a squealing brake, as unstable solutions in linear models show an increasing amplitude above all boundaries with time while the real brake squealing is represented by a more or less stationary behavior with distinct frequencies and finite amplitudes. Therefore, the behavior observed in the brake squealing can only be represented by nonlinear models [10]. Hereby, nonlinearities limit the increasing vibration caused by the self-excitation finally ending in a limit cycle [10, 11]. Several attempts have been made in the past years to describe these effects and to investigate the resulting effects, e.g. [12-19]. These attempts are essential for several reasons. One reason is that the nonlinearity limiting the limit cycle could be a key for avoiding squealing, i.e. if this nonlinearity could be designed in a way that the amplitudes of the limit cycles are irrelevant for noise, the problem of brake squeal would be solved. Another reason is that nonlinearities can play a key role, when it comes to the desired predictive character of the simulation methods. In [11] it is shown that the mode shape belonging to the largest positive eigenvalue real part is not necessarily the one occurring in the limit cycle, as nonlinearities may limit that mode much earlier than another mode shape with a smaller positive real part.

As a conclusion, nonlinearities are essential for the description of brake squeal and may play a key role for its suppression. Nevertheless, as the description above makes obvious, nonlinearities, if actually considered, are so far considered in detail only at one place of the simulation process, namely in limiting the increasing vibrations. Another obvious point, where nonlinearities play a role, is in determining the equilibrium position. Here, in general, only one equilibrium position and its dependency on parameters such as brake pressure are considered, while the immanent nonlinearities could also result in multiple equilibrium positions with the same parameters due to different initial conditions. This fact is completely ignored in state of the art simulations. Most people having done experiments with squealing brakes may have experienced that a squealing brake can be brought to silence or *vice versa*, if the positions of some parts of the brake are manipulated e.g. by pressing temporarily a screwdriver on them. Sometimes it is visible with the naked eye that the position of the brake parts is not the same after this manipulation as it was before, so that a new equilibrium position has been reached, possibly with decisive influence on the noise behavior.

For both types of above mentioned influences of nonlinearities, the initial conditions play an essential role in determining which solution appears. With respect to the limit cycle, the initial conditions decide in the case of coexistent stable limit cycle and stable trivial solution about the appearance of squealing [20], but the same happens, if different equilibrium positions are possible due to nonlinearities, where the stability behaviors may differ from each other. In reality, nonlinearities affect the noise behavior in both cases and the dependence on the initial conditions is the explanation why brake squeal sometimes occurs and sometimes not for the same operation conditions.

The present paper aims to investigate experimentally the influence of the actually engaged equilibrium position on the noise behavior and, therefore, to investigate another influence of nonlinearities on the brake squeal. In reality, the engaged equilibrium position is determined during the process of applying the brake pressure. This process is highly nonlinear especially due to the new contacts occurring therein. Therefore, it is highly probable that different equilibrium positions can be established depending on the initial conditions, respectively the state of the brake before the brake pressure is applied. Additionally, there might be some influence of external excitation on the engaged equilibrium position.

As experiments show, the concept of one engaged stationary equilibrium position is an idealization in simulations, as these equilibrium positions may also change periodically during the turning of the disk due to disk wobbling or other imperfections. Nevertheless, the following investigations show that there is significant dependence of the occurrence of squealing on the (medium) absolute and relative positions of the brake parts; they also show that significant different positions are possible even for constant operation parameters.

In the metrological investigation it is necessary to consider that the changes in the positions are slow (quasi static) and with respect to the displacement in the order of 0.1 millimeters or more. Squealing, however, has usually a much smaller displacement amplitude (µm range or smaller) and it occurs at frequencies in the range of approximately 1 to 16 kHz. While conventional set-ups regarding the investigation of brake squeal are focused on measuring these high frequency vibrations by using accelerometers or laser vibrometers, other methods must be established for measuring the equilibrium positions.

The paper is structured as follows. First, the developed test bench is presented. The test setup comprises an optical 3D measuring system filming the brake. The position data of respective parts can be determined using digital image correlation (DIC). This method

allows the determination of the position of many points on the structure for low frequencies (quasi static) and comparatively large displacements. Based on this, two test series are presented. Test series number one is used to investigate whether changes in equilibrium position can occur under almost identical parameters for braking torque, speed and temperature and whether these changes have a significant influence on the squealing behavior. In a second test series, what is investigated is the extent to which an increasing braking torque influences the equilibrium position. The results are collected and discussed in a manner which illustrates the essential influence of the equilibrium position on the squealing behavior.

2. Experimental Setup

The main task of the experimental setup is to detect differences in the equilibrium position of the examined floating caliper disk brake while the disk is rotating at a specific speed and a specific brake pressure is applied. Especially the brake components carrier, caliper and pad are considered. Furthermore, the test bench must be able to detect squealing events and to record the corresponding parameters, namely rotational speed, brake torque, respectively, brake pressure and temperature.

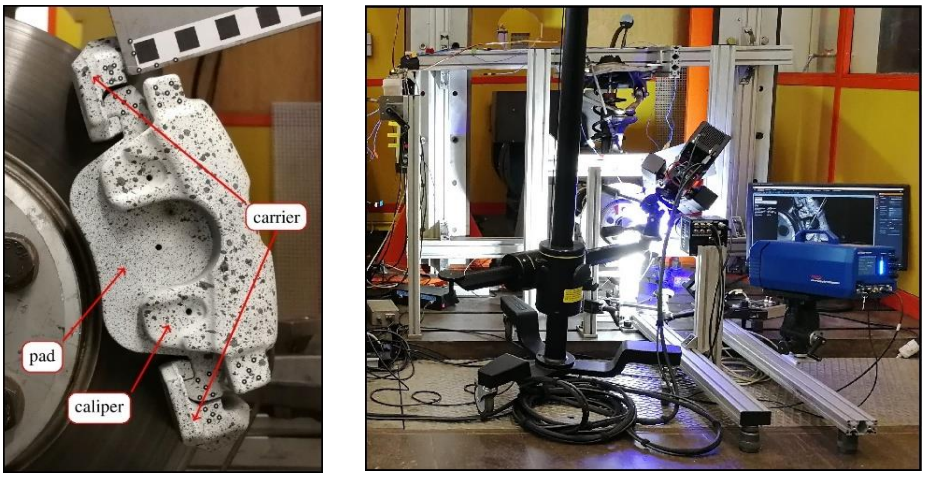

Fig. 1 Left: main components, i.e. the carrier, caliper and pad of the investigated industrial floating caliper brake [21]. Right: overview of the test bench with mounted brake and optical 3D measuring system [22]

Fig. 1 shows one of the brake test benches at MMD TU Berlin, which was already used in several prior works, e.g. [11]. It includes an industrial floating caliper disk brake driven by an electric motor *via* the original drive shaft from the inner side. To allow for a wider range of equilibrium positions, the clamp connecting the carrier and the caliper (Fig. 16 left) in the serial setup was omitted in these two first test series. Nevertheless, similar effects are also observed when the clamp is mounted, as demonstrated in a third test series. The entire control of the brake pressure and rotational speed is done manually.

Compared to industrial test benches this set up does not allow the investigation of high rotational speeds or high torques and, therefore, it is not capable of analyzing the brake performance. Nevertheless, brake squeal generally requires only low rotational speeds and torques. The main advantage of this set-up is that most parts of the brake are perfectly accessible for optical measurements. Here, this accessibility is used to observe one side of the brake using a GOM Aramis optical 3D measuring system, determining the position of the brake parts with a high spatial resolution.

This 3D measuring system essentially consists of two cameras and a lighting system. It enables the capturing of grayscale images with 25 frames per second (fps) and a resolution of 2752 by 2200 pixel. Self-adhesive point markers with an inner diameter of 1.5 mm are attached to the components carrier, pad and caliper (see Fig. 2 right). The image sequence recorded by the 3D-system makes it possible to determine the spatial movement of these point markers by using DIC for homologous point tracking in all three dimensions. The equipment used is state of the art.

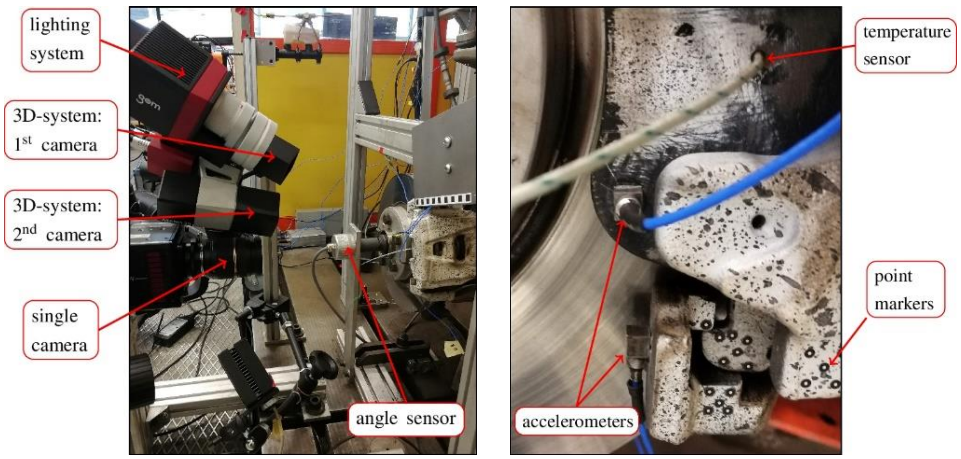

Fig. 2 Details of the test bench [23]. Left: 3D-system, single camera, angle sensor and mounting for the coordinate system. Right: accelerometers, temperature sensor and point markers

Nevertheless, the computation algorithm as described in [24] for the determination of displacement data shall be briefly sketched. The glued-on point markers are identified and tracked *via* image recognition techniques. The center of the point determines the position of the measurement point. Therefore, the tracking resolution is in subpixel accuracy and for this setup in the order of approximately 5µm [25, 26]. The subpixel resolution is possible since the points consist of several pixels and, therefore, the center can be interpolated. Each camera records a separate image sequence, and the point tracking is also done separately. According to [27] the data from both cameras can be combined to determine the 3D position of the point markers.

Beside the 3D-system there is also a single camera, Photron FASTCAM Mini AX100 with an applied resolution of 896 by 768 pixel, for possible 2D measurements. This camera is utilized to display a live image of the brake to adapt or record certain initial conditions

before the brake pressure is applied. By overlaying the live image and a previously stored reference image it is possible to (approximately) reproduce spatial initial conditions. Fig. 3 shows two examples of this live image. In both cases this is overlaid with a reference image. On the left hand side, the live image is almost the same as the reference. Therefore, it is hard to recognize that two images are overlaid. This also means that in this case the conditions stored in the reference image are almost identical to the conditions shown in the live view. On the right hand side, it can be seen that there are two images overlaid (especially in the region highlighted with the red circle). This indicates that the actual conditions differ from the reference conditions.

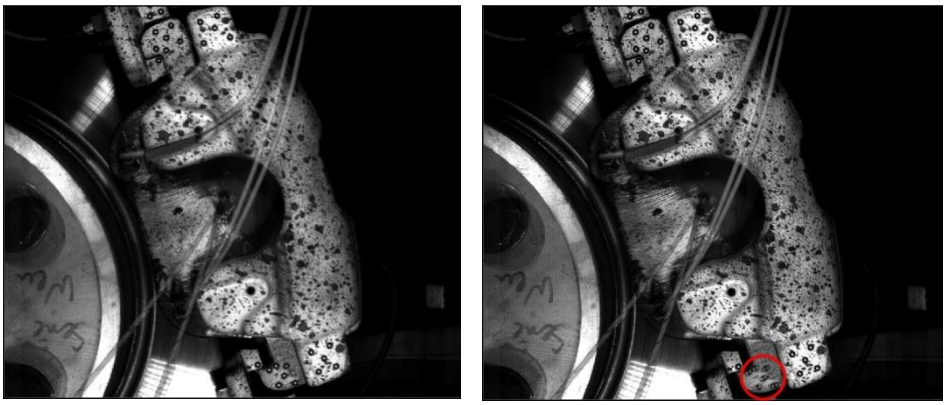

Fig. 3 Exemplary field of vision of the single camera live image overlaid with a previously stored reference image. Left: high agreement between live and reference image. Right: relatively high divergence of the two positions visible by naked eye especially in downside part marked by the red circle

Furthermore, four triaxial accelerometers are attached to the carrier and to the pad to investigate the high frequency oscillations of the brake components and to detect whether the brake is squealing or not. The alignment takes place tangentially, radially and normal to the disk plane, respectively.

The effective braking torque is determined by the strain gauges attached to the drive shaft. The values of temperature, rotational speed and rotational angle of the brake disk are measured by additional sensors. All signals are recorded simultaneously and synchronized with the information from the image sequence.

3. MEASUREMENTS

To determine experimentally whether different initial conditions result in different equilibrium positions and if those changes have a significant influence on the squealing behavior, two test constellations are conducted. In the first constellation (test series 1), multiple tests are performed where the operation parameters like braking torque, rotational speed and temperature are equal for all tests and constant during the actual test phase. When assuming a constant friction coefficient, the brake pressure is proportional to the braking torque. Since the braking torque can be measured more accurately than the brake pressure,

the brake torque is considered in the following. Since all operating parameters are kept constant, only different initial conditions or the positions of the brake components before the brake pressure is applied are possible. Therefore, test series 1 is used to determine whether these initial conditions have a significant influence on the positions respectively the equilibrium positions of the brake components after the brake pressure is applied and whether these differences have a significant influence on the squealing behavior. Parts of the measurement setup and evaluation procedure were developed in the master's thesis of the second author.

Each test run includes three steps. First, an initial position is adjusted manually before the brake pressure and the rotational speed are applied. The live view of the single camera and the overlaid reference image (Fig. 3) are used for this purpose. Then the rotational speed of the disk is adjusted, and the brake pressure is slowly increased to a specific level. To ensure that during all tests the temperature of the disk is the same, it is measured by an infrared sensor. In the case of a temperature lower than the target one, a warm-up cycle is done until the target temperature is reached. Finally, the actual test starts, where all data are recorded in a time interval of 31.24 s while the brake pressure and rotational speed are constant. The time interval of 31.24 s results from the maximum number of images which can be stored uncompressed by the camera. In the second constellation (test series 2), the main procedure is equal except that the braking pressure is continuously increased during the recoding of the data. In total, 146 measurements were carried out, 70 for test series 1 and 76 for test series 2.

4. Evaluation Procedure

The evaluation procedure is shown by two example measurements from test series 1. The two chosen measurements are denoted by M1 with audible squealing and M2 without audible squealing, respectively.

During a single measurement, 782 individual images are recorded with a frame rate of 25 fps whereby the positions of all point markers are determined for each image. All calculated position data refer to the coordinate system shown in Fig. 4, where the directions are oriented in tangential $\mathbf{e}_x$, radial $\mathbf{e}_y$ and out of plane $\mathbf{e}_z$ direction. The position of the i-th point P_i can be written as

$$\vec{x}_i = \begin{pmatrix} x_i \\ y_i \\ z_i \end{pmatrix}. \tag{1}$$

The position and orientation of the coordinate system are defined by additional point markers which are attached to a frame mounted to the base of the test bench. Therefore, slight changes in the camera position do not influence the origin of the reference coordinate system and the position of the points on the brake is always measured relatively to this inertial coordinate system. Fig. 5 shows the position results for the two considered measurements M1 and M2 for P_1, P_2 and P_3.

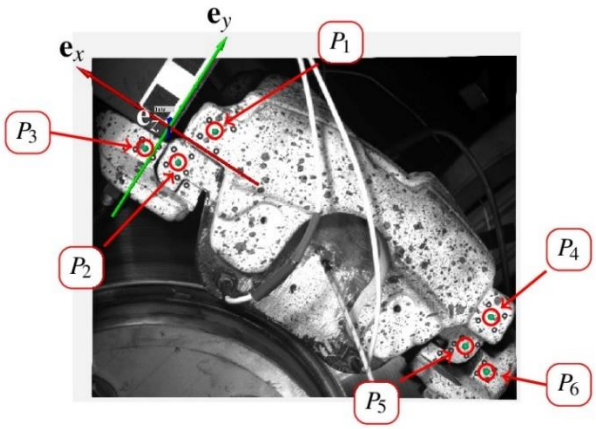

Point	Position on the brake
P_1	carrier top
P_2	pad top
P_3	caliper top
P_4	carrier bottom
P_5	pad bottom
P_6	caliper bottom

Fig. 4 Example of an image recorded by the optical 3D measuring system. Applied coordinate system and measurement points $P_1$to P_6 (green dots) according to the table on the right. The brake disk rotates counterclockwise

It should be emphasized that the visible fluctuations in the positions in Fig. 5 are not related to brake squeal, as the displacement amplitudes here are much higher and the frequencies are much lower compared with the squeal. Squeal only takes place in M1, while M2 is silent. Instead of this, as will be shown later, the fluctuations visible in Fig. 5 are related to the actual rotational angle of the disk and its origin can, therefore, be related to the brake disk wobbling or other out-of-roundness imperfections of the brake. Focusing on squealing, which takes place at much higher frequencies than the turning of the disk, it can even be said that the equilibrium position might change periodically during the turning of the disk. The effect - observed very often during our measurements and in general - is that the brake does not squeal permanently while turning, but only at certain ranges of rotational angles; or in the case of permanent squealing the intensity varies with the rotational angle.

As a result, the concept of one stationary equilibrium position applied in simulations can hardly be found in measurements. Instead, brake squeal is a low amplitude high frequency vibration around an actual position. This position is varying itself in amplitudes of higher order of magnitudes with the frequency of disk turning. Additionally, as Fig. 5 demonstrates, there are significant differences in the positions possible even for the same operation parameters, and these differences in position, as will be shown later on in several measurements, can make a difference between squeal (M1) and non-squeal (M2)!

This is not only true for the absolute, but also for relative positions of the brake parts as will be shown in the following. Based on the positions considered so far, also the absolute value of the relative position, i.e. distances

$$\Delta_{ij} = \left|\vec{x}_i - \vec{x}_j\right| \tag{2}$$

between two points P_i and P_j can be determined.

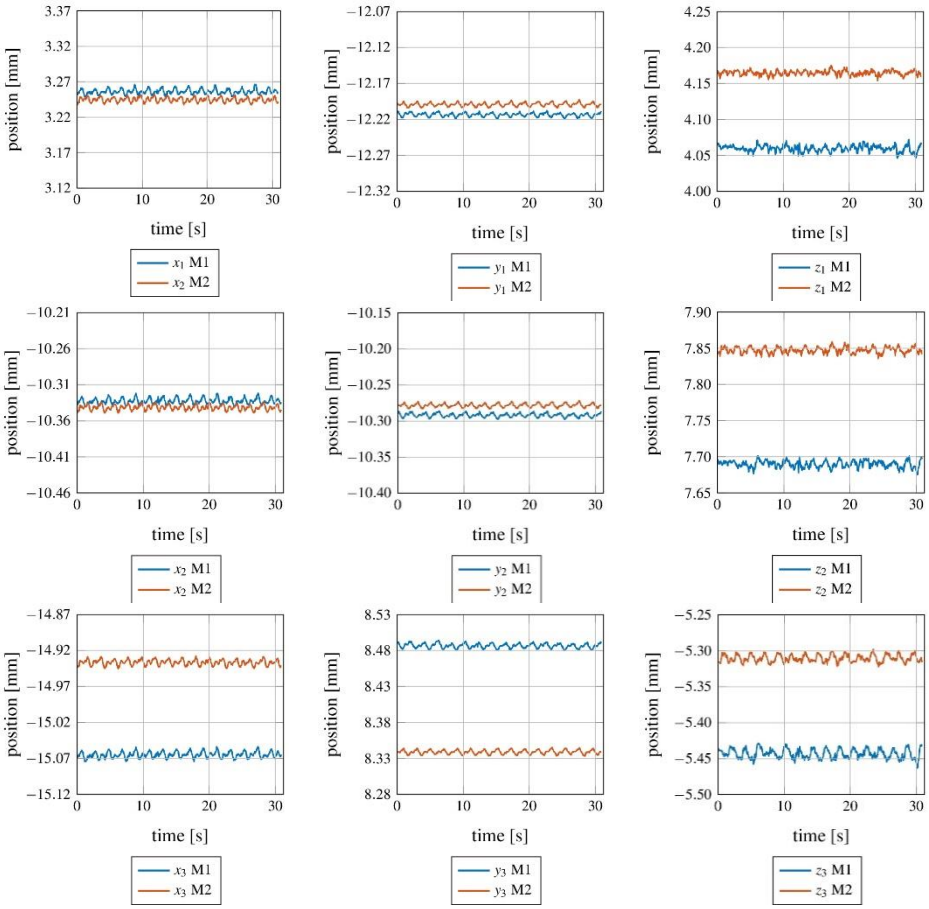

Fig. 5 Positions of P_1 (top), P_2 (middle) and P_3 (bottom). Measurement M1 (squealing) in blue and Measurement M2 (no squealing) in orange. The medium positions in case of audible squeal (M1) and without squeal (M2) differ significantly

Assuming that the parts of the brake are approximately rigid with respect to the displacement scale considered in the positions, the actual absolute position can be determined by the positions of the measured points. Nevertheless, the relative positions or their absolute value of the connected brake parts are considered in the following. The following results, in fact, show that significant differences in relative positions can be observed in squealing and non-squealing cases, so that even the condensed information from Eq. (2) seems to be sufficiently significant. Corresponding results for the two cases M1 and M2 are shown in Fig 6.

Besides the positions, brake torque M and rotational angle φ of the brake disk are also measured during the test period. Compared to the position measurements that are recorded at every 0.04 s, the measurement set-up allowed much higher sampling rates for these signals. Therefore, the mean value of these signals is calculated at every 0.04 s.

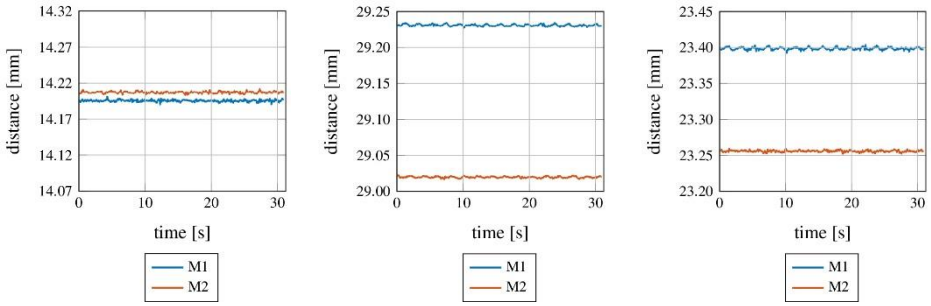

(a) Δ_{12} (b) Δ_{13} (c) Δ_{23}

Fig. 6 Distances Δ_{23} according to Eq. (2) for M1 (squeal, blue) and M2 (no squeal, orange). Significant differences of the distances can be observed between the squealing (M1) and the non-squealing case (M2)

In addition to these parameters, it is necessary to determine whether the brake is squealing or not. Therefore, the data recorded by the accelerometer at the bottom of the carrier (see Fig. 2 right) are used while the data of other accelerometers would also have been suitable for this task. In Fig.7 the time series of this signal are shown for test M1 (left) with audible squealing and test M2 (right) without squealing. It can be clearly seen that the amplitude is higher while the brake is squealing. However, several previously performed tests have shown that a simple consideration of the amplitude is not sufficient to determine a squealing event since the amplitude varied also due to other parameters like brake pressure or rotational speed. Therefore, it is hard to define a specific threshold for the amplitude which indicates whether squealing occurs or not. To overcome this issue the almost mono-frequent characteristics of the brake squeal are taken into account. To integrate this in the evaluation process a specific band acceleration level L_a is defined according to [28] as

$$L_a = 20 \cdot \log_{10} \sum_i 10^{L_{a,i}0.2} \text{ dB} \quad \text{with:} \quad a_0 = 5 \cdot 10^{-5} \frac{\text{m}}{\text{s}^2}$$
$$L_{a,i} = 20 \cdot \log\left(\frac{a_i}{a_0}\right) \text{ dB}, \tag{3}$$

where a_i is the value of the i-th measuring point in the power spectrum in a range of ± 20 Hz around the previously determined squealing frequency of 2.65 kHz. Reference acceleration a_0 is chosen in the way that the minimum band acceleration level in a series of measurements results in 0 dB. This specific band acceleration level is very sensitive to the frequencies close to the squealing one; hence a better squealing indicator than the overall amplitude or intensity of the signal. From a practical point of view, it should be mentioned that a significantly different squealing frequency that could have occurred during the measurements would have been audible and would therefore have been taken into account. However, it must be considered that this indicator will fail if the brake squeals at a significantly different frequency. Nevertheless, as the test bench needs permanent supervision this would probably be recognized.

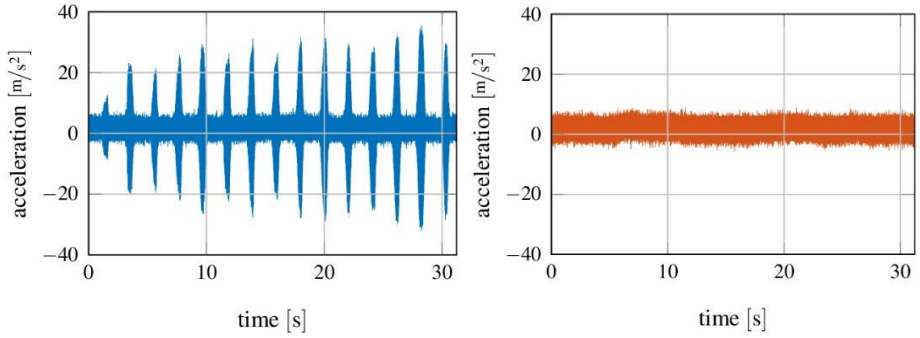

Fig. 7 Time signals of the accelerometer at carrier bottom used for the detection of squeal. Left M1 with audible squealing events and right M2 without

The time series of the accelerometers are recorded with a sample rate of 30 kHz during the test. Since the optical measurement system has a frame rate of 25 fps the position information is recorded at every 0.04 s. To calculate the corresponding band acceleration level also within this time interval, the time series of the acceleration data is divided into synchronous time sequences of 0.04 s. Then the results in each interval are transferred to the frequency domain by using the Fast Fourier Transformation. As a result, the power spectrum of the acceleration related to each image taken by the camera with 25 fps is available. Two plots of exemplary frequency bands for the band acceleration level are shown in Fig. 8.The red colored area (± 20 Hz around 2.65 kHz) indicates the values used for the calculation of the band acceleration level. Fig. 9 shows the band acceleration level for the complete measurement M1 (left) and M2 (right). It should be noticed that in the case of squealing (M1) L_a is much higher but varies with a constant period. This period correlates with the rotational speed of the brake. By defining

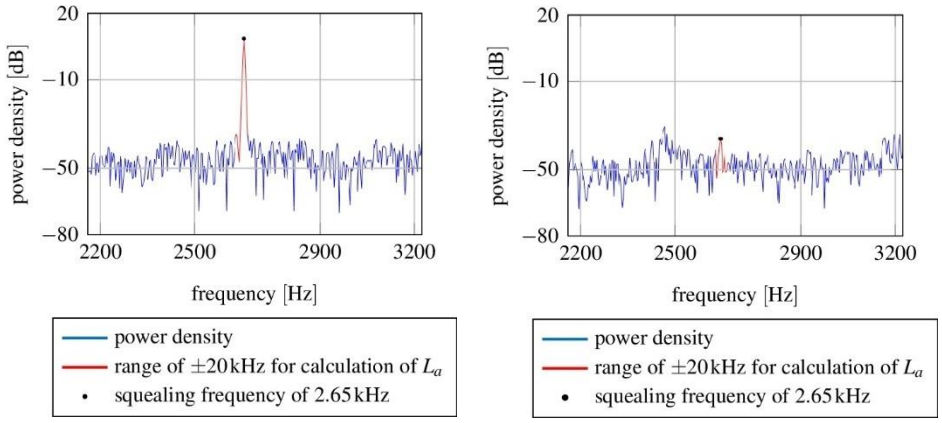

Fig. 8 Examples of a 0.04 s time sequence transferred to the frequency domain for M1(left, with squealing event) and M2 (right, without squealing event). The power spectrum is shown in blue and the range of ± 20 Hz around the squealing frequency considered for calculating L_a according to Eq. (3) is shown in red. The black dot marks the previously determined potential squealing frequency of 2.65 kHz. [29]

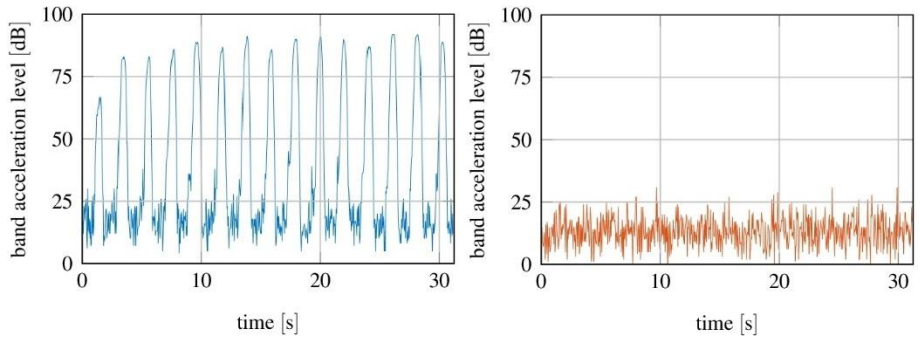

Fig. 9 Band acceleration level La according to Eq. (3) for the measurement M1 (left) and M2 (right)

a threshold value of 60 dB for the band acceleration level, which indicates that the brake squeals; when this value is exceeded, the figure shows that the squeal is not constant but appears repetitively with each revolution of the brake disk. This was also audible during the tests, where the squealing event was not continuous but repeated with every rotation of the disk.

To investigate this phenomenon in more details Fig. 10 shows the band acceleration level and the braking torque as a function of the rotational angle of the disk. It can be seen that both values are strongly related to the rotational angle, but the torque does not differ significantly between the squealing and the non-squealing cases. This indicates that the disk includes some imperfections, such as wobbling, which has an influence on the brake torque and on the squealing condition. Since the aim of the first test series is to identify the influence of the actual relative position on the squealing behavior and this relative position is changing with the rotational angle, the rotational angle is also considered for the entire test duration.

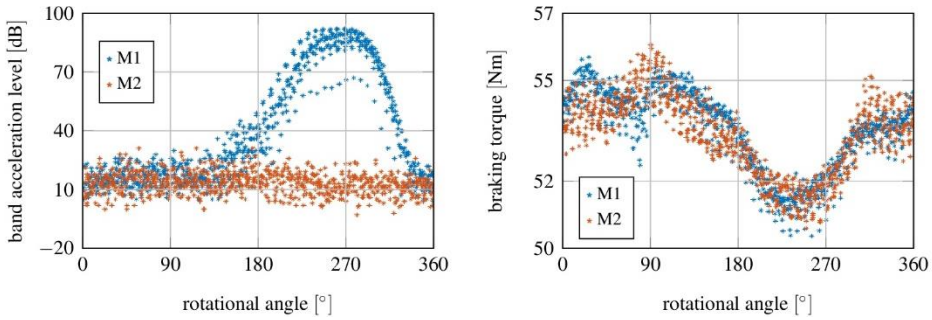

Fig. 10 Band acceleration level L_a as squealing indicator (left) and braking torque (right) as function of rotational angle φ for the measurements M1 (blue) and M2 (orange)

To visualize the influence of the position changes on the squealing behavior, the band acceleration level as the squeal indicator is plotted in color as a function of the rotational angle and relative position. Fig. 11 shows this for the two measurements M1 and M2. Each point in the plot represents the data recorded every 0.04 s.

Each vertical path corresponds to one test series. It is noticeable that the variation of the relative position during each individual measurement is small compared to the differences between both measurements. One series of relative positions is related to squeal while the others are related to non-squeal. The only differences are varied initial conditions, while all the operation parameters are kept constant. Since only two tests are considered in the plot, large white areas are present indicating that these relative positions were not reached.

In the following, the complete test series will be discussed, while using the way of representation as in Fig. 11. As written earlier, the initial position is fixed manually with the help of a single camera which only allows a rough and not very precise determination of the initial position. It should also be mentioned that, in general, the initial positions are far away from the actual equilibrium positions, as the brake components are elastically hinged and, therefore, move with displacement amplitudes of several millimeters, if the brake torque is applied. Nevertheless, the following results show that a large range of positions can be reached but only some of them make the brake susceptible to noise.

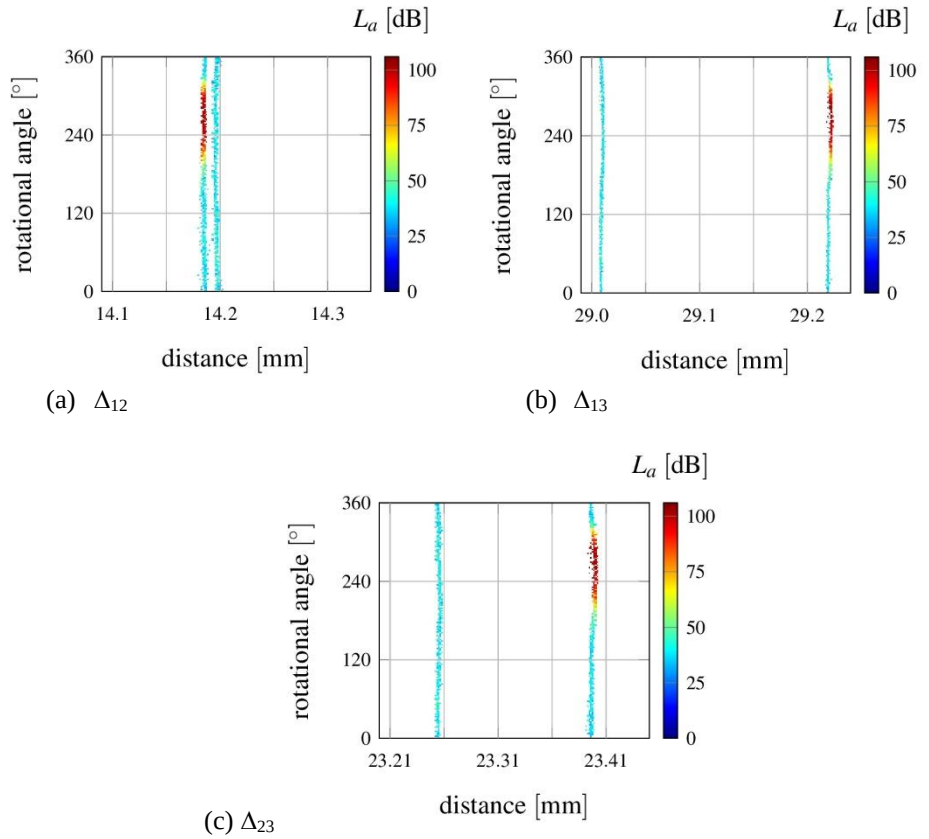

Fig. 1 Band acceleration level L_a (squealing indicator) according to Eq. (3) as function of the distances for both measurements M1 (with squealing event) and M2 (without squealing event)

5. RESULTS

The results for the complete test series 1 are shown in Figs. 12 and 13. Following the description of Fig. 11, each plot shows the band acceleration level according to Eq. (3), which is visualized by color as a function of the rotational angle of the disk and the relative position between two specific points on different parts of the brake. In test series 1 all investigated parameters are identical for all measurements and constant during each test session. Hereby the braking torque is $M \approx 53$ Nm, the temperature $T = 31$ °C and the rotational speed $v = 28.8$ rpm. Only the initial conditions are varied manually by adjusting them to the reference image, so that finally varying position series are kept. This shows that the relative positions of the parts carrier, caliper and pad vary, and that multiple equilibrium positions are possible due to different initial conditions.

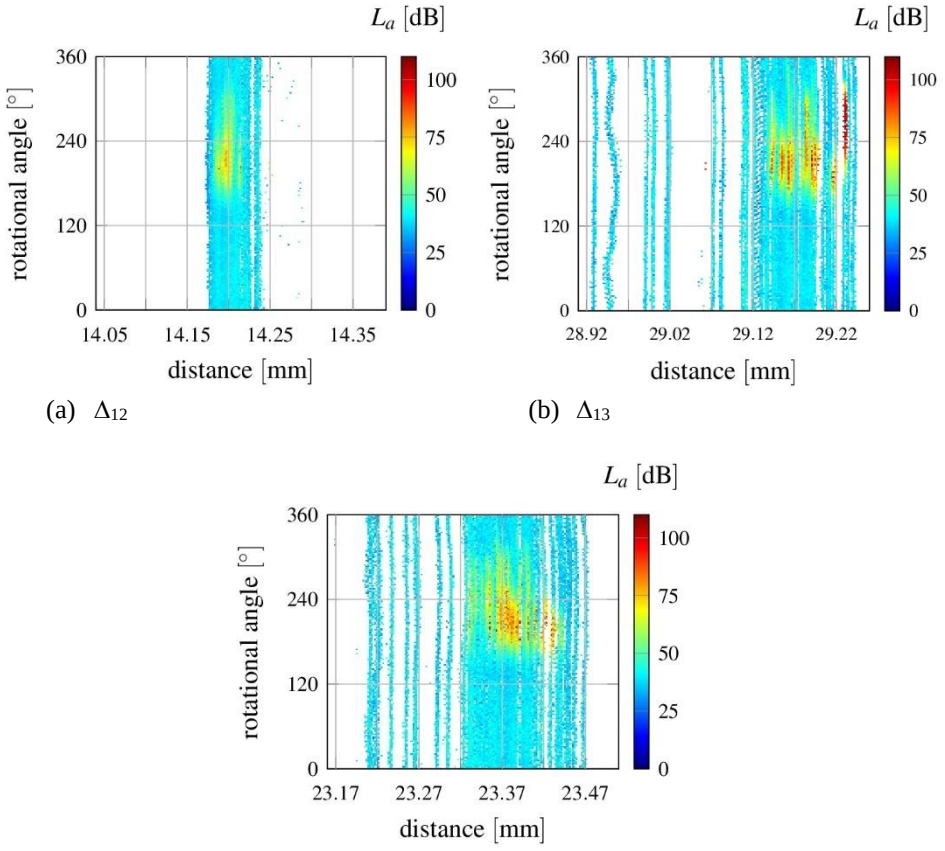

(a) Δ_{12} (b) Δ_{13}

(c) Δ_{23}

Fig. 12 Band acceleration level L_a as function of distances Δ_{12}, $\Delta_{13}$and Δ_{23} according to Eq. (2) and rotational angel φ for constant braking torque M, rotation speed v and temperature T for the upper 3 point markers P_1, P_2 and P_3. Red areas indicate squealing. All 70 measurements of test series 1 are included in each image.

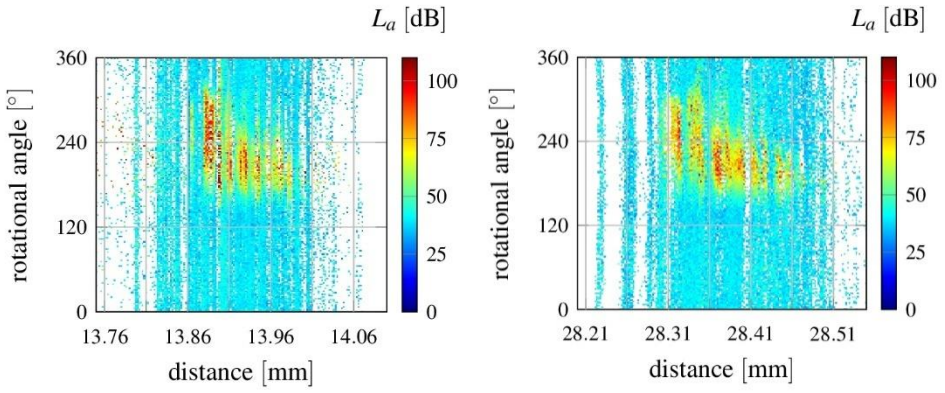

(a) Δ_{45} (b) Δ_{46}

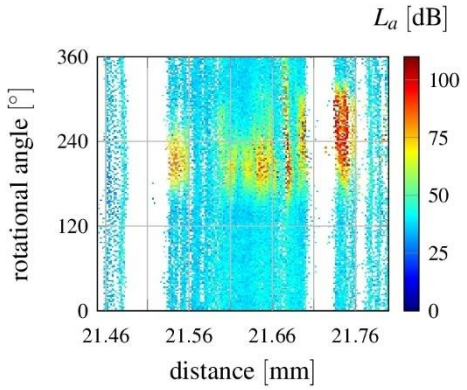

(c) Δ_{56}

Fig. 13 Band acceleration level La as function of distances Δ_{45}, Δ_{46} and Δ_{56} according to Eq. (2) and rotational angel φ for constant braking torque M, rotation speed v and temperature T for the bottom 3 point markers P_4, P_5 and P_6. Red areas indicate squealing. All 70 measurements of test series 1 are included in each image [30].

It is noticeable that for a certain rotational position of the disk the squealing tendency depends only on the relative position. There are distinct areas (blue color only) where the brake never squealed and significant areas (red color) where the brake always squealed. These distinct areas, where the squealing indicator is high, show the strong dependence of the squealing behavior on the relative positions.

In test series 2 the braking torque respective the brake pressure is increased slowly by hand (see Fig. 14) during the test procedure. Temperature and rotational speed remain unchanged. Again, at the beginning of each measurement, the initial conditions were varied relative to the reference image as in test series 1. The potential squealing frequency is again 2.65 kHz. Due to the limited recording time, less data per braking torque are available. Nevertheless, the data is sorted by braking torque at every 5 Nm[1].

[1]The data points are divided into braking torque interval of 0.5 Nm.

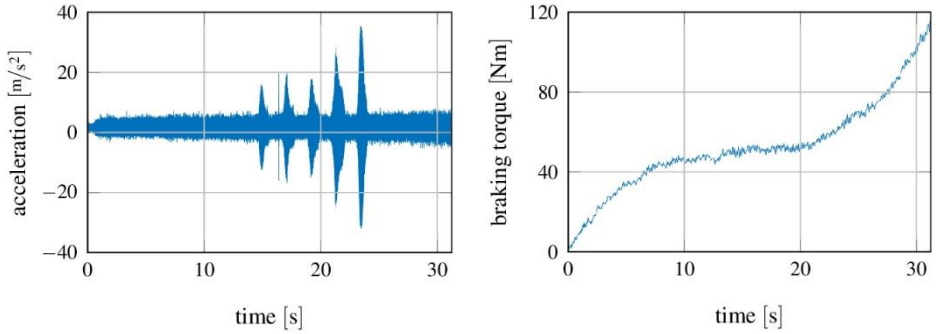

Fig. 14 Exemplary time profiles for quasi-static increase of the braking torque (right) with corresponding band acceleration level L_a (left) for test series 2

Fig. 15 shows again the band acceleration level as a function of the rotational angle and the distance. When a braking torque of approx. 50 Nm is reached, a red-colored area with a high band acceleration level is visible and so is an area of the positions which have led to squealing. There are also areas that are permanently without squeal. This result is consistent with the one determined from test series 1 (Fig. 13b) as the torque is $M \approx 53$ Nm in that case. If a braking torque level of approx. 65 Nm is exceeded, the squealing disappears completely for all investigated initial conditions. Test series 2 shows the well-known influence of the braking torque on the squealing behavior. In connection with equilibrium positions, however, it shows that only the combination of specific relative positions, which is dependent on the respective initial condition and the transient process (e. g. applying the corresponding braking pressure), leads to squealing. For example, distances Δ_{46} between 28.35 µm and 28.45 µm did not cause any squeal until a certain brake pressure was reached. Due to the elastic connecting elements between the components of a brake, it is obvious that the brake components shift significantly when a braking torque is applied.

It should be noted that during the measurement test series 1 and 2 and, as already mentioned in the introduction of the experimental setup, the clamp (see Fig. 16 left) connecting the carrier and the caliper was removed. In the passenger car brakes, such a part is sometimes used for functional reasons, but not specifically to avoid noise. Based on the previous results such a clamp might restrict the range of possible equilibrium positions and, therefore, be capable of avoiding squealing. To investigate whether the mounting of the clamp has a corresponding effect on the investigated brake a third test series was conducted. In this test the clamp was installed while the test procedure was otherwise similar to test series 1. The results in Fig. 16(right) show in fact that the clamp fixes the components in such a way that only smaller changes, e. g. in distance Δ_{46}, are possible. Nevertheless, the main properties that different positions are possible for constant operation parameters while some of them are resulting in squealing and some not, are still valid.

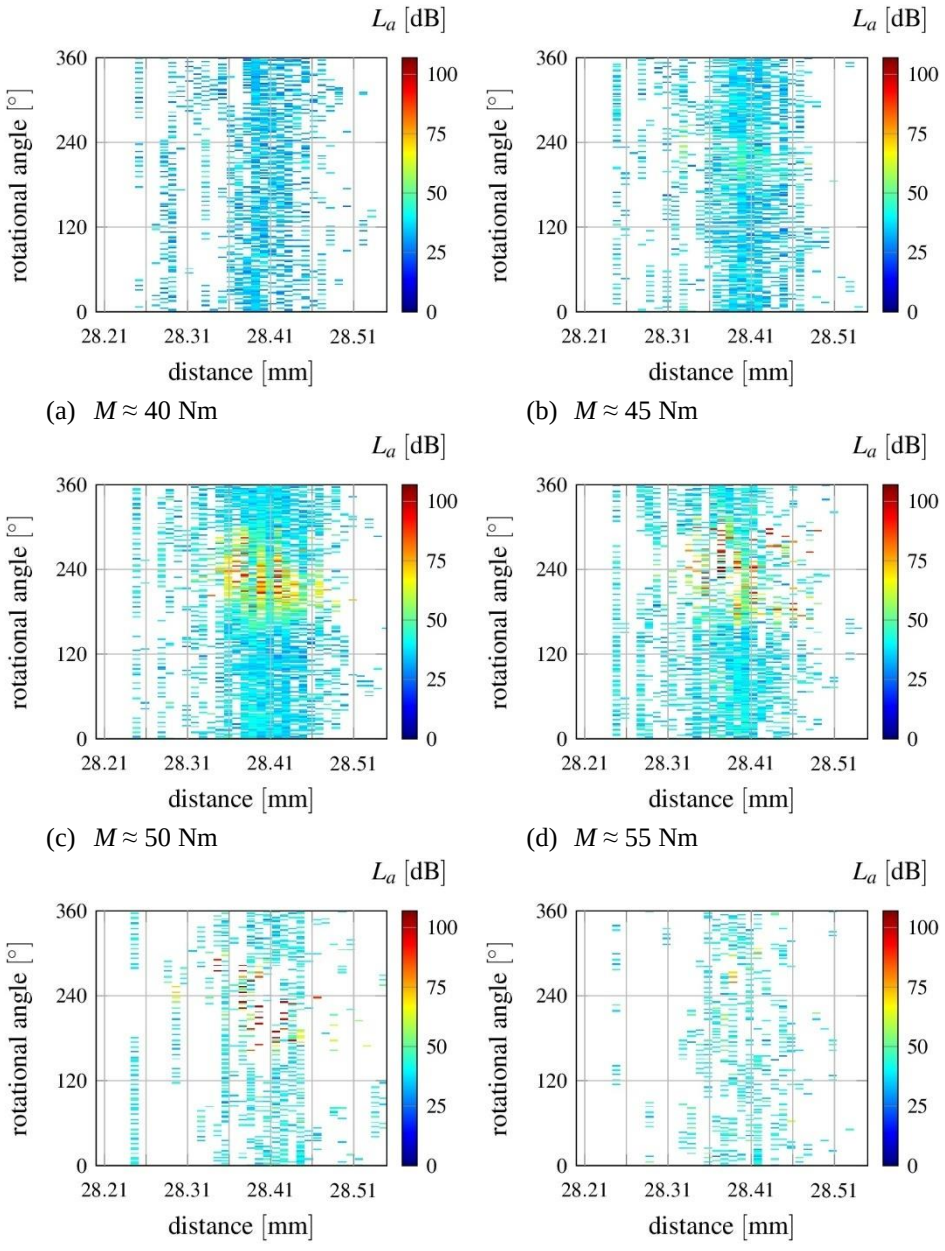

(a) $M \approx 40$ Nm (b) $M \approx 45$ Nm

(c) $M \approx 50$ Nm (d) $M \approx 55$ Nm

(e) $M \approx 60$ Nm (f) $M \approx 65$ Nm

Fig. 15 Band acceleration level L_a as function of distance Δ_{46} and rotational angel φ in the case of increasing braking torque M at constant rotational speed v and temperature T (test series 2). Red areas indicate squealing. All 76 measurements of test series 2 are included in each image

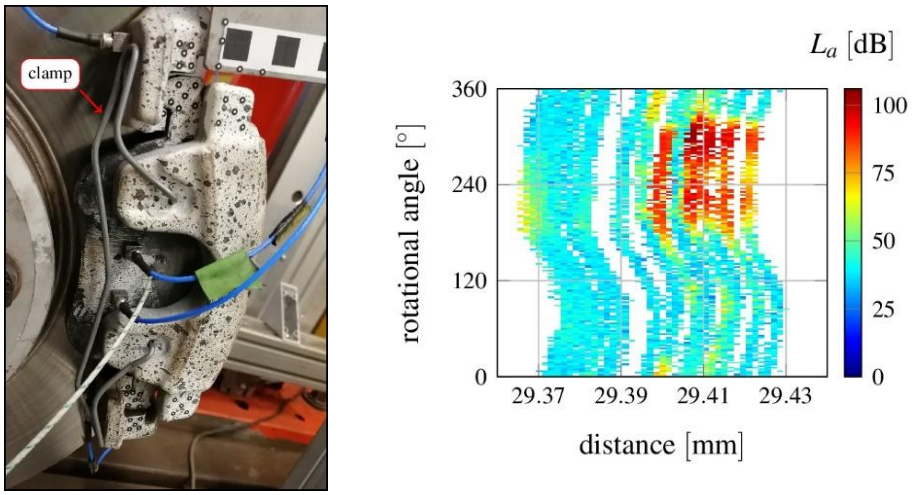

Fig. 16 Left: clamp mounted for the 3rd test series. Right: Band acceleration L_a as function of distances Δ_{46} according to Eq. (2) and rotational angel φ for constant braking torque M, rotation speed v and temperature T with mounted clamp (test series 3). Red areas indicate squealing

6. Summary and Outlook

State of the art simulations of the brake squeal do not provide a predictive tool and extensive experimental investigations are still necessary to find appropriate designs. Actual investigations on this topic focus on the consideration of nonlinearities but do so in most cases by trying to model and simulate the limit cycle behavior representing squeal. In contrast to this, the actual paper considers the influence of the equilibrium position engaged during stationary braking due to the transient process. In fact, the elements of the brake, namely the carrier, caliper and pad, are highly nonlinear elastically coupled and allow for multiple equilibrium positions as is demonstrated in the present paper. It is also demonstrated that the engaged position may have a decisive influence on the occurrence of squeal, i. e., depending on which equilibrium position is engaged, the brake squeals or not for the same operation parameters. For the purpose of these investigations an experimental setup and a corresponding analyzing method are established to measure the position engaged by the brake components using an optical 3D-measuring system. These experimental results indicate observations that most people doing experimental work with brake noise probably have made: squealing can be stopped or initiated e. g. by pressing on brake parts with a screw-driver (i.e. possibly manipulating the equilibrium position) and for same operation conditions brake squeal sometimes occurs and sometimes not. The (relative) positions of brake parts are hereby in general not considered.

Assuming that the results are representative, the conclusions are that essential effects for brake squeal are actually not considered in state of the art industrial and actual scientific investigations, which is a possible explanation for the poor predictive character of actual simulation tools. Consequences for simulations should be that the possibility of multiple

equilibria has to be considered. For stability analysis, the equations of motion then must be linearized with respect to these multiple possible equilibria with the ultimate possibility, that for some equilibria significant instability may occur, and for others not, even in the case of constant operation parameters. On the other hand, consequences for the design of a silent brake could be that the enforcement of specific equilibrium positions could be helpful in avoiding squealing. Finally, a consequence for experimental investigations of the NVH behavior of brakes could be that stationary positions of brake parts should be measured by default.

Acknowledgements: *The authors thank the Extrusion Research and Development Center of the TU Berlin, in particular Sören Müller and René Nitschke for the provision of the 3D system for our measurements and support during commissioning.*

REFERENCES

1. Kinkaid, N.M., O'Reilly, O.M., Papadopoulos, P., 2003, *Automotive disk brake squeal*, Journal of Sound and Vibration, 267, pp. 105-166.
2. Cantoni, C., Cesarini, R., Mastinu, G., Rocca, G., Sicigliano, R., 2009, *Brake comfort - a review*, Vehicle Systems Dynamics, 47(8), pp. 901-947.
3. Dunlap, K.B., Riehle, M.A., Longhouse, R. E., 1999, *An investigative overview of automotive disc brake noise*, SAE transactions, pp. 515-522.
4. Chen, F., Abdelhamid, M.K., Blaschke, P., Swayze, J., 2003, *On automotive disc brake squeal part III test and evaluation*, SAE Technical Paper, 2003-01-1622.
5. Stump, O., Könning, M., Seemann, W., 2017, Transient Squeal Analysis of a Non Steady State Maneuver, EuroBrak.
6. Stump, O., Nunes, R., Häsler, K., Seemann, W., 2019, *Linear and nonlinear stability analysis of a fixed caliper brake during forward and backward driving*, Journal of Vibration and Acoustic, 141(3), pp. 2161-2170.
7. Bonnay, K., Magnier, V., Brunel, J.F., Dufrénoy, P., De Saxce, G., 2015, *Influence of geometry imperfections on squeal noise linked to mode lock-in*, Internal Journal of Solids and Structures, 75/76, pp. 99-108.
8. Intes, 2012, *PERMAS User´s Reference Manual*, Stuttgart: INTES Publication No. 450.
9. Ouyang, H., Nack, W., Yuan, Y., Chen, F., 2005, *Numerical analysis of automotive disc brake squeal: a review*, International Journal of Vehicle Noise and Vibration, 1(3-4), pp. 207-231.
10. Hochlenert, D., von Wagner, U., 2011, *How do nonlinearities influence brake squeal?*, SAE Technical paper 2011-01-2365, pp. 179-186.
11. Gräbner, N., 2016, *Analyse und Verbesserung der Simulationsmethode des Bremsenquietschens*, PhD Thesis, Technische Universität Berlin, Germany, 114 p.
12. Tiedemann, M., Kruse, S., Hoffmann, N., 2015, *Dominant damping effects in friction brake noise, vibration and harshness: the relevance of joints*, Proceeding of the Institute of Mechanical Engineers Part D: Journal of Automobile Engineering, 229(6), pp. 728-734.
13. Martin, G., Vermot des Roches, G., Balmes, E., Chancelier, T., 2019, *MDRE: An efficient expansion tool to perform model updating from squeal measurements*, Proceedings of EuroBrake 2019.
14. Tison, T., Heussaff, A., Massa, F., Turpin, I., Nunes, R.F., 2014, *Improvement in the predictivity of squeal simulations: Uncertainty and robustness*, Journal of Sound and Vibration, 333(15), pp. 3394-3412.
15. Kruse, S., Tiedemann, M., Zeumer, B., Reuss, P., Hoffmann, N., Hetzler, H., 2015, *The influence of joints on friction induced vibration in brake squeal*, Journal of Sound and Vibration, 340, pp. 239-252.
16. Koch, S., Gräbner, N., Gödecker, H., von Wagner, U., 2017, *Nonlinear multiple body models for brake squeal*, PAMM, 17(1), pp. 33-36.
17. Massi, F., Baillet, L., Giannini, O., Sestieri, A., 2007, *Brake squeal: Linear and nonlinear numerical approaches*, Mechanical Systems and Signal Processing, 21(6), pp. 2374-2393.
18. Oberst, S., Lai, J.C.S., 2015, *Nonlinear transient and chaotic interactions in disc brake squeal*, Journal of Sound and Vibration, 342, pp. 272-289.
19. Nacivet, S., Sinou, J.-J., 2017, *Modal amplitude stability analysis and its application to brake squeal*, Applied Acoustics, 116, pp. 127-138.

20. Gräbner, N., Tiedemann, M., von Wagner, U., Hoffmann, N., 2014, *Nonlinearities in friction brake NVH-experimental and numerical studies*, SAE Technical Paper, 2014-01-2511.
21. Koch, S., 2021, *Main components floating caliper brake*, Dataset: doi:10.6084/m9.figshare.13663556.v1 (https://figshare.com/articles/figure/Main_components_floating_caliper_prake_pdf/13663556,last access: 11.02.2021)
22. Koch, S., 2021, *Overview test bench with optical 3D measuring system*, Dataset: doi:10.6084/m9.figshare.13663622.v1 (https://figshare.com/articles/figure/Overview_test_bench_with_optical_3D_measuring_system_pdf/13663622,last access: 11.02.2021)
23. Koch, S., 2021, *Details test Bench with optical 3D measuring system*, Dataset: doi:10.6084/m9.figshare.13663631.v1 (https://figshare.com/articles/figure/Details_test_Bench_with_optical_3D_measuring_system/13663631, last access: 11.02.2021)
24. GOM GmbH, 2016, *Technische Dokumentation: Grundlagen der digitalen Bildkorrelation und Dehnungsberechnung*. *V8 SR1*, Braunschweig, Germany.
25. Bing, P., Hui-Min, X., Bo-Qin, X., Fu-Long, D., 2006, *Performance of sub-pixel registration algorithms in digital image correlation*, Measurement Science and Technology, 17(6), pp. 1615-1621.
26. Sutton, M. A., Orteu, J. J., Schreier, H., 2009, *Image correlation for shape, motion and deformation measurements: basic concepts, theory and applications*, Springer Science & Business Media, 321 p.
27. Sutton, M.A., Yan, J.H., Tiwari, V., Schreier, H. W., Orteu, J.J., 2008, *The effect of out-of-plane motion on 2D and 3D digital image correlation measurements*, Optics and Lasers in Engineering, 46(10), pp. 746-757.
28. Beranek, L.L., Ver, I.L., 1992, *Noise and vibration control engineering: principles and applications*, John Wiley & Sons, 966 p.
29. Koch, S., 2021, *Power spectrum with squealing frequency*, Dataset: doi:10.6084/m9.figshare.13663694.v1 (https://figshare.com/articles/figure/power_spectrum_with_squealing_frequency/13663694/1, last access: 11.02.2021)
30. Koch, S., 2021, E*quilibrium positions*, Dataset: doi:10.6084/m9.figshare.13673059.v2 (https://figshare.com/articles/figure/equilibrium_positions/13673059/2, last access: 11.02.2021)